NASA TECHNICAL NOTE

NASA TN D-3942

NASA TN D-3942

IMPROVING PERFORMANCE OF FACE CONTACT SEAL IN LIQUID SODIUM (400° TO 1000° F) BY INCORPORATION OF SPIRAL-GROOVE GEOMETRY

by Lawrence P. Ludwig, Thomas N. Strom, Gordon P. Allen, and Robert L. Johnson

Lewis Research Center
Cleveland, Ohio

NATIONAL AERONAUTICS AND SPACE ADMINISTRATION • WASHINGTON, D. C. • MAY 1967

NASA TN D-3942

IMPROVING PERFORMANCE OF FACE CONTACT SEAL IN LIQUID SODIUM (400° TO 1000° F) BY INCORPORATION OF SPIRAL-GROOVE GEOMETRY

By Lawrence P. Ludwig, Thomas N. Strom, Gordon P. Allen, and Robert L. Johnson

Lewis Research Center
Cleveland, Ohio

NATIONAL AERONAUTICS AND SPACE ADMINISTRATION

For sale by the Clearinghouse for Federal Scientific and Technical Information
Springfield, Virginia 22151 – CFSTI price $3.00

IMPROVING PERFORMANCE OF FACE CONTACT SEAL IN LIQUID SODIUM (400° TO 1000° F) BY INCORPORATION OF SPIRAL-GROOVE GEOMETRY

by Lawrence P. Ludwig, Thomas N. Strom, Gordon P. Allen, and Robert L. Johnson

Lewis Research Center

SUMMARY

Conventional face contact seal performance was improved by incorporation of the spiral-groove geometry. Both conventional face contact seals and seals with spiral grooves were used to seal liquid sodium at a pressure of 20 pounds per square inch gage (13.8 N/cm^2 gage), and a sliding velocity of 79 feet per second (24 m/sec). In comparison with conventional face contact seals, seals with spiral grooves had negligible leakage. The wear and contact patterns indicated that the spiral-groove seal operated with separation of the sealing surfaces, which is necessary for long life.

Successful low-leakage operation was not achieved with conventional face contact seals having carbide seal seats and nosepieces (hard on hard). Thermal and pressure distortions caused edge contact, wear, and scoring. Conventional face contact seals having seal seats and nosepieces with wear-in properties (soft on hard) showed more leakage than those with carbide sealing surfaces.

INTRODUCTION

Shaft seals for containment of alkali liquid metals have applications in space power conversion systems (ref. 1). The design of these seals presents formidable problems because of high liquid temperatures (to 1337° F (725° C) for low-power systems) (ref. 2), lightweight requirement, and extremely low leakage-rate allowance of the order of several pounds per year. In addition, a high degree of reliability must be maintained for periods of 1 to 3 years of essentially unattended operation. Additional application areas for alkali metal shaft seals are found in pumps for liquid-metal flight control systems (ref. 3) and in homopolar electric machines utilizing liquid metals to transfer high-density currents (ref. 4).

The face contact seal has not been successfully applied in long-term operation as the primary seal in direct contact with alkali liquid metals. However, it is potentially a compact and complete seal system and therefore is worthy of investigation.

For long life (1 to 3 yr) and high reliability, the seal must operate with separation between the sliding surfaces (seal dam). Sliding contact of solid surfaces would probably be permissible at startup and shutdown. Separation of sliding surfaces of an argon gas seal has been accomplished by employing wavy sealing surfaces which produce a hydrodynamic lift (ref. 5). In addition to surface waviness, other possible features responsible for, or contributing to, hydrodynamic separation are (1) cavitation caused by minute surface discontinuities and roughness (ref. 6), (2) axial vibration, or squeeze-film effect (ref. 7), (3) nutating motion of the seal nosepiece (ref. 7), and (4) thermal wedge effect (ref. 8).

It is herein suggested that by incorporating the viscoseal principle (in the form of a spiral groove) into the face seal, sealing surface separation and low-leakage rates can be obtained simultaneously. (Reference 9 presents a theoretical analysis of the viscoseal principles.) The sealing-surface separation at operating speeds will ensure long seal life, and the pumping effect of the spiral-groove geometry will provide low leakage rates.

The objectives of this work were to investigate (using liquid sodium as the sealed fluid) the following:

(1) Sealing and hydrodynamic effects of the spiral groove used in conjunction with the face contact seal

(2) Leakage rates of conventional face contact seals without spiral grooves

(3) Wear characteristics of various candidate seal material combinations in conventional face contact seals

Since surface damage must be avoided on seal startup and shutdown, attention was given to sliding materials suggested by the literature. (Materials are discussed in the TEST SEALS section of this report.) This investigation was conducted with a bellows face contact seal in direct contact with liquid sodium under pressure. Surface speeds to 79 feet per second (24 m/sec) and temperatures to 1000° F (538° C) were investigated.

APPARATUS AND PROCEDURE

Figure 1 is a schematic diagram of the seal assembly and experimental apparatus. The rotating seal seat is attached to the horizontal shaft which is supported radially and axially by externally pressurized gas bearings (not shown). The shaft is driven by a variable speed electric drive and step-up transmission; shaft speed is monitored by a magnetic pickup. The seal housing and bellows assembly is mounted in a containment and support vessel that is filled with liquid sodium and pressurized to the operating

pressure. The seal nosepiece, which is piloted by three pins (figs. 1 and 2), is held against the seal seat by a hydraulic force and by a bellows spring force. Relative motion occurs between the sealing surfaces. The bellows, besides providing a mechanical spring force, also serves as a secondary seal and allows axial motion of the seal nosepiece. Roller bearing support (not shown) for the containment and support vessel permits axial movement for controlling the amount of bellows spring force. This axial movement is controlled by means of an air-operated piston mounted outside the enclosure (fig. 3). The enclosure is pressurized slightly above ambient pressure with argon to ensure an inert environment around the containment and support vessel.

The sodium-supply and leakage-rate monitoring system is shown schematically in figure 3. Before transferring sodium, the enclosure, the containment vessel, and the leakage monitoring tank are successively evacuated and purged with argon several times to remove air. In order to transfer the sodium, the leakage monitoring tank is vented, the sample bypass leg is closed, and the reservoir is pressurized. Sodium is passed through the 20- and 5-micron filters and then to the containment vessel. The reservoir temperature is held at approximately 220° F (104° C), which is high enough to ensure transfer but low enough to allow sodium oxide precipitation and filtration. Oxide solubility is 20 parts per million at 220° F (104° C) (ref. 10). After the containment vessel is filled, the leakage-rate monitoring tank is filled to the predetermined level. The argon pressure can be remotely changed to provide various pressure differentials across the seal. Sodium temperature in the containment and support vessel is maintained by a surrounding induction coil (fig. 3). Seal leakage results in a lowering of the sodium level (changing the float position) in the leakage-rate monitoring tank. The float position is monitored by a differential transformer, the output of which is continuously recorded.

The sodium system is cleaned by the "hot flushing" technique. In this hot flushing procedure, the system is filled with sodium, soaked at operating temperatures, and then the sodium is passed back to the reservoir through the sample leg bypass line. This process is repeated several times. The oxide content is determined from a sample trapped between valves A and B (fig. 3) in the sample bypass line. The oxide content, determined by the mercury amalgamation method (ref. 11), ranged between 10 and 100 parts per million.

TEST SEALS

Seal Geometry

Flatness of the seal seat and nosepiece was held within one light band (23×10^{-6} in. or

6×10^{-5} cm). Figure 4, a typical seal seat flatness check, shows the interference pattern obtained with an optical flat placed on top of a seal seat. The parallel line pattern indicates that the flatness in the sealing area is within one light band. As a check on assembly distortions, the flatness was examined after the seal seat was clamped into position and it usually was less than two light bands. Figure 5 shows a typical surface roughness check and corresponding photomicrograph of a tungsten carbide seal seat. The photomicrograph shows the presence of surface scratches which were not removed in the final lapping operation, and the surface roughness check indicates an average peak-to-valley distance of less than 4×10^{-6} inch (10^{-5} cm).

Seal Material Selection

No exact rules exist for selecting sliding material combinations for sodium or sodium-potassium environments. The obvious requirement is that of chemical compatibility with the alkali metal at the seal operating temperature.

The material selection for the rubbing faces is made more difficult by the poor boundary lubricating properties of sodium. As pointed out in reference 2, sodium will reduce surface oxides which are normally present on metals and which are beneficial in hindering adhesion of sliding surfaces in the boundary lubrication regime. In addition, the viscosity of sodium (a significant factor in both hydrodynamic and boundary lubricating regimes) at the boiling point is 2×10^{-8} reyn (2.9×10^{-6} (lb)(sec)/ft^2 or 0.14 cP) (ref. 2), which is only 1/100 of the viscosity of SAE 10 oil at room temperature.

Investigators have tested many rubbing combinations in sodium and in sodium-potassium alloys. The results of these tests show that the majority of successful rubbing combinations employ a hard alloy cermet or oxide for one or both of the rubbing surfaces (refs. 12 to 14). As an example, in an evaluation test of material wear and adhesion in sodium at temperatures to 1000° F (538° C), the harder combinations showed better resistance to adhesive wear than did the softer material combinations (ref. 13).

Good results were obtained with soft on hard combinations in reference 15, which reports substantial wear-in of copper on tungsten carbide, and of copper on tungsten, and the subsequent development of a hydrodynamic lift component (due to wear-in) capable of supporting 10 000 pounds per square inch (6900 N/cm^2) in a sodium-potassium alloy at 482° F (250° C).

Reference 16 suggests that the formation of sodium molybdate (Na_2MoO_4) films was beneficial in reducing friction and wear of a molybdenum couple in sodium. However, a thermochemical analysis indicates that the oxides of molybdenum are chemically unstable

in liquid sodium except in the presence of large concentrations of sodium oxide. Reference 17 also investigated the effects of the surface films on sliding couples in sodium and concluded that the friction behavior depends to a large extent on whether the sodium dissolves the surface oxide or reacts with the metal and surface oxide to form a protecting film. Another form of surface protection is found in solid films of calcium fluoride - barium fluoride (CaF_2-BaF_2); these solid films are reported in reference 18 to be effective lubricants in liquid sodium at temperatures to 1000° F (538° C).

Seal Installation Procedure

The seal components and housing parts were degreased, scrubbed with levigated alumina, and cleaned ultrasonically in a chlorofluorocarbon before installation in the rig. This procedure produced seal components free of hydrocarbon films and polishing media. The seal seat face runout was limited to a maximum of 0.0005 inch per inch (0.0005 cm/cm) of diameter and averaged approximately 0.0003 inch per inch (0.0003 cm/cm) of diameter. By calculation, the inertia forces at operating speeds due to this runout are not sufficient by themselves to lift the seal nosepiece out of contact with the seal seat. Before sodium was introduced, the seal was checked for proper assembly by pressurizing with argon and measuring the leakage.

Bellows Calibration

Both the bellows spring force and the pressure thrust force contribute to the net loading at the sealing surfaces. Figure 6 shows a typical calibration of the bellows spring force against bellows compression. The amount of bellows compression was held at 0.040 inch (0.10 cm) during operation. This amount of compression resulted in a 3.14-pound (14.0-N) bellows spring force, which tended to close the gap between the sealing surfaces.

Pressure Balance

The principle of seal pressure balance is reviewed herein since a pressure balanced seal is usually necessary for long life, high-speed applications. The thrust force due to pressurizing the bellows can be completely or partly balanced out; as a result, none or only a small fraction of the bellows thrust force acts on the sealing surfaces. The principle of pressure balancing is illustrated in figure 7 for an internally pressurized seal in which the bellows has been replaced by a piston ring ("O" ring) and spring for purposes

of illustration. If the piston ring is placed on the nosepiece outside diameter (fig. 7(a)), the sealed pressure force (rectangular area) exceeds the gap pressure force (triangular area) and the nosepiece is forced against the seal; this is a pressure-loaded seal. If the piston ring is placed on the nosepiece inside diameter, the sealed pressure force no longer acts on the nosepiece and the gap pressure force opens the seal (fig. 7(b)). However, a diameter can be selected for the piston ring such that the sealed pressure force nearly balances the gap pressure force (fig. 7(c)); this is a pressure-balanced seal. The degree of pressure balance selected depends on the degree to which the gap pressure profile can be predicted and controlled. A complete description of the seal balance must consider the following:

(1) Closing force changes due to shift of the bellows mean effective diameter with pressure

(2) Pressure profile changes under the seal dam due to distortion, surface waviness, and nonparallel sealing surfaces (dam)

(3) Spring force of the bellows

(4) Development of pressures under the seal dam due to hydrodynamic effects and fluid phase change effects

(5) Inertia forces due to seal seat runout

The preceding factors vary widely among different applications, and selection of seal balance is largely dependent on experience.

Seal Gap

The success of a conventional face contact seal depends largely on what occurs at the seal gap (sliding surfaces). The leakage rate varies with the cube of the gap height (fig. 7(c)), and lubrication and dynamics within the gap determine power loss and wear life. The following are various possible modes of operation:

(1) Continuous or near-continuous rubbing contact between solid surfaces (This mode of operation is suitable for finite life or low-speed applications. Solid film lubricants such as calcium fluoride - barium fluoride (ref. 18) and reaction films such as reported in reference 16 are important here.)

(2) Separation of the sliding surfaces (except, perhaps, at startup or shutdown) (This mode of operation is necessary for long life and high-speed applications.)

(3) Operation under conditions intermediate between (1) and (2)

To meet the high seal reliability and low-power-loss requirements of the space power system, the seals must operate with separation of the sliding seal surfaces. Basically, this interface separation can be achieved by hydrostatic forces, by hydrodynamic forces, or by combined hydrostatic and hydrodynamic forces. Hydrostatic seals

would have too much leakage for the space power application and are beyond the scope of this report. Therefore, the objective is to produce separation of the sealing surfaces by hydrodynamic forces.

In general, theories and explanations for separation of sealing surfaces are based on the hydrodynamic lifting effects of minute surface discontinuities, cavitation, surface waviness, axial vibration, thermal wedges, and nutation of the seal nosepiece. These microscopic geometric and interface dynamics are difficult to control and to produce consistently. Further, the separation produced by these hydrodynamic effects usually leads to leakage.

A better approach is to use a seal geometry which will produce hydrodynamic separation forces in conjunction with pumping action to inhibit leakage. The spiral groove fits these requirements. This was, therefore, the approach taken in this investigation. The spiral groove can be incorporated in the face contact seal and offers the theoretical possibility of zero leakage with sealing surface separation (zero wear). Figures 8 and 9 show a typical spiral-groove face used in this evaluation.

RESULTS AND DISCUSSION

Carbide Seal Rings (Hard on Hard Combination) In Conventional Face Contact Seals

Carbide nosepieces mated to carbide seal seats were evaluated because it has been reported (refs. 12 to 14) that the majority of successful combinations for sliding contact in alkali metals employ a carbide for one or both surfaces. Table I lists the carbide materials evaluated, the pertinent parameters, and the results. In general, operation with a carbide nosepiece mated to a carbide seal seat was not successful. The leakage rates were either initially excessive or increased with running time to high levels because of sealing surface wear.

Thermal distortion. - The wear patterns indicated that significant thermal distortion occurred in each carbide combination evaluated (table I). Distortions are induced by thermal gradients in the seal seat and nosepiece and produce contact initially at the inner diameter of the sealing surfaces, as shown exaggeratedly in figure 10. Since carbide materials are very hard (85 to 94 Rockwell A) and have high elastic moduli (56×10^6 to 91×10^6 psi, 39×10^6 to 63×10^6 N/cm^2), the wear-in and conformability properties are practically nonexistent, and thermal distortions become significant factors in contact stress and in the lifting-force pressure profile across the sealing surfaces. The magnitude of the thermal distortions is determined by the spherical shape assumed by the seal seat and nosepiece (fig. 10) when a temperature gradient exists. When end constraints are

TABLE I. - CARBIDE SEAL SEAT AND NOSEPIECE COMBINATIONS (HARD ON HARD), OPERATIONAL PARAMETERS, AND LEAKAGE RATES

[Sliding speed, 79 ft/sec (24 m/sec).]

Run	Seal nosepiece				Seal seat				Sodium temperature		Sealed pressure		Operating time, hr	Leakage rate				Oxygen content, ppm	Condition of seal surfaces after run
	Matrix		Binder		Matrix		Binder							$in.^3/hr$		cm^3/hr			
	Carbide	Weight percent	Metal	Weight percent	Carbide	Weight percent	Metal	Weight percent	°F	°C	psig	N/cm^2 gage		Start	End	Start	End		
1	Titanium carbide - niobium carbide - tantalum carbide	80	Cobalt	20	Tungsten carbide	91	Cobalt	9	1000	538	50	34.5	4.5	1.1	1.5	18	25	---	Unsatisfactory
2	Tungsten carbide	91	Cobalt	9	Titanium carbide - niobium carbide - tantalum carbide	80	Cobalt	20	1000	538	30	20.7	19.0	1.8	2.7	30	45	---	Unsatisfactory
3											30	20.7	4.0	.2	3.3	3	55	---	Unsatisfactory
4											60	41.4	7.0	.6	2.1	10	35	28	Unsatisfactory
5					Tungsten carbide	100	----------	--	1000	538	5	3.5	1.5	---	0.6	--	10	17	Unsatisfactory
6	Titanium carbide - niobium carbide - tantalum carbide	80	Cobalt	20	Tungsten carbide	100	----------	--	1000	538	30	20.7	1.0	1.7	17.1	28	280	39	Unsatisfactory
7	Tungsten carbide	89	Cobalt	11	Tungsten carbide	100	----------	--	500 to 650	260 to 343	10	6.9	1.5	---	24.4	--	400	99	Unsatisfactory
8		100	------	--		100	----------	--	800 to 1000	427 to 538	50	34.5	7.0	0.2	2.4	3	40	---	
9		100	------	--		89	Cobalt	11	540 to 600	282 to 316	40	27.4	18.0	.2	6.1	4	100	---	
10		89	Cobalt	11		---	Cobalt and chromium	--	400 to 1000	204 to 538	40	27.4	19.3	0	1.7	0	28	100	
11	Titanium carbide - niobium carbide - tantalum carbide	80	Cobalt	20	Tungsten carbide	91	Cobalt	9	1000	538	50	34.5	20.0	0.6	0.6	10	10	67	Satisfactory

neglected, reference 19 gives the radius of the curvature of this sphere as

$$\frac{1}{r} = \frac{\alpha \Delta t}{h} \tag{1}$$

where r is the radius of the curvature of the sphere, α the thermal expansion coefficient, Δt the axial temperature gradient, and h the axial ring thickness. Since the thermal gradient $\Delta t/h$ is inversely proportional to the thermal conductivity β,

$$\frac{1}{r} \propto \left(\frac{\alpha}{\beta}\right) \tag{2}$$

Therefore, the magnitude of thermal distortion increases as the ratio of thermal expansion coefficient over the thermal conductivity increases. Table II lists this ratio for several candidate seal materials; the larger values indicate greater distortion.

These comparative values suggest that the carbides and molybdenum are candidate seal materials. For example, molybdenum should have 1/20 of the distortion of 347 stainless steel. However, despite the favorable α/β, the carbide and molybdenum seal rings indicated excessive distortion as evidenced by edge contact.

An example of excessive distortion is given in figure 11 which shows the condition of a titanium carbide nosepiece after a short period (40 min) of operation in sodium at a temperature of 740° F (393° C) and a sliding velocity of 79 feet per second (24 m/sec).

TABLE II. - THERMAL DISTORTION CRITERIA

Material	Expansion coefficient, α		Conductivity,[d] β		Ratio of expansion coefficient to conductivity, α/β	Relative rating
	in./(in.)(°F)	cm/(cm)(°C)	Btu/(hr)(ft)(°F)	cal/(sec)(cm)(°C)		
347 Stainless steel	[a]10.30×10^{-6}	[a]5.72×10^{-6}	11.9	0.049	0.868×10^{-6}	20
Aluminum oxide (Al_2O_3)	[b]4.10	[b]2.28	5.8	.024	.707	$16\frac{1}{2}$
Titanium carbide (20-percent cobalt binder)	[b]4.20	[b]2.33	17.9	.074	.234	$5\frac{1}{2}$
Tungsten carbide (binderless)	[b]3.25	[b]1.81	35.0	.145	.093	2
Tungsten carbide (6-percent cobalt binder)	[b]2.85	[b]1.58	44.5	.184	.064	$1\frac{1}{2}$
Molybdenum	[c]3.20	[c]1.78	74.0	.306	.043	1

[a] 32° to 932° F (0 to 500° C).
[b] Room temperature to 842° F (450° C).
[c] 68° to 1060° F (20° to 571° C).
[d] At 842° F (450° C).

Except for the portion near the inner edge, the majority of the surface shows no evidence of rubbing contact. Under the condition of thermal distortion, the inner edge would be expected to contact first. However, as shown in figure 4, the inner and outer edges have a slight dropoff because of the lapping operation. This dropoff also occurred in the nosepiece; thus, contact occurs first at a diameter slightly larger than the inside diameter. Figure 12 shows the wear pattern on a tungsten carbide seal seat which was typical of hard on hard combinations. At various points around the seal seat a surface profile trace was taken across the sealing surfaces, and a photomicrograph of the corresponding area was matched to the surface profile trace. Distortions caused initial contact near the inside diameter of the sealing dam on the nosepiece. The wear, heaviest near the inside diameter of the wear track, decreased to near zero at the outside diameter of the wear track. A corresponding wear pattern occurred on the seal nosepiece as shown in figure 13.

In general, effective lubrication of the carbide seal seats and nosepieces was not obtained. In addition to wear (figs. 12 and 13), the surfaces showed evidence of heat checking (fig. 14), which is indicative of excessive sliding surface temperatures.

Since thermal distortions were found to be a primary concern in seal operation, an analytical investigation was conducted to determine thermal gradients in the seal seat. Figure 15 shows the calculated thermal maps for two of the shapes of seal seats employed. The approximate distortion for both seal seats was 2×10^{-4} inch (5×10^{-4} cm). The thermal gradients in the nosepiece were calculated to be equally as severe as in the seal seats. Distortions of this order cannot be accommodated by materials of high hardness and high modulus; therefore, edge loading is inevitable.

Leakage. - Leakage rates of the carbide combinations (table I) were not predictable; in general, they were initially high and increased to excessive levels after short running periods. One run, with a titanium carbide nosepiece mated to a tungsten carbide seal seat, did not show an increase in leakage rate, and this was attributed to development of a hydrodynamic lubricating film between the sealing surfaces. Inspection revealed that the surfaces were in good condition but had nonuniform contact (fig. 16) because of surface waviness. This slight surface waviness could have developed a hydrodynamic film which would account for the constant leakage rate of 0.61 cubic inch per hour (10 cm^3/hr) and the good surface condition. A leakage rate of 0.61 cubic inch per hour (10 cm^3/hr) is excessive for the space power system application, but for applications in which this rate is tolerable, the beneficial effect of surface waviness should not be overlooked.

Figure 17 shows the leakage trends which were evident throughout the evaluation. The leakage increased with speed because of the combined effect of centrifugal force and larger average gap produced by seal runout. The increase in leakage with pressure is expected, but the minimums exhibited at certain pressures are unexplained.

Conventional Face Contact Seals With One Sliding Surface Having a Conformability Property (Soft on Hard Combination)

Thermal distortion proved to be a major problem with seals having carbide seal seats sliding against carbide nosepiece rings (hard on hard combinations); therefore, various seal ring materials having a wear-in or conformability property were evaluated. Table III includes the seal ring materials evaluated, pertinent parameters, and results.

Foam metal rings impregnated with calcium fluoride - barium fluoride. - Nickel-base alloy and nickel foam metal impregnated with calcium fluoride - barium fluoride showed the desired conformability to thermal distortion. Sliding contact over the full width of the sealing surface was obtained by the wear-in process as shown in figure 18. The tungsten carbide mating nosepiece surface showed no indication of scoring, metal transfer, or adhesive wear. Thus the calcium fluoride - barium fluoride impregnated material was performing the lubricating function as pointed out in reference 18. However, the leakage rates were excessive (table III) for the space power type of application.

Copper nosepieces and molybdenum seal seats. - In a further effort to attain a wear-in or conformability property, copper and molybdenum nosepieces were run against tungsten carbide and against each other. (Reference 15 reported a wear-in property with copper mated to tungsten carbide, and reference 16 reported formation of beneficial surface films on molybdenum in sodium.) The copper and tungsten carbide combination showed no evidence of scoring or metal transfer. However, the sodium leakage rate was excessive (table III), and the wear-in process did not reduce seal leakage. The molybdenum and tungsten carbide combination showed scoring and adhesive wear of the molybdenum surface (fig. 19), and the leakage was excessive. A combination of copper sliding against molybdenum showed extreme surface distress and operated only for 3 minutes.

Face Seal With Spiral Grooves

Face seals were constructed with spiral grooves on the high pressure side of the sealing surfaces (dam). One assembly incorporated grooves on the nosepiece (fig. 8); grooves on the seal seat were also evaluated. The geometric details of the spiral grooves are shown in figure 9. The motion of the rotating seal seat causes the spiral grooves to produce an inward pumping action against leakage of sodium.

Leakage and wear. - Table IV lists the leakage results and operating conditions. A copper nosepiece (fig. 8) with spiral grooves and a seal seat of tungsten carbide operated in liquid sodium for 4 hours at 20 pounds per square inch gage (14 N/cm^2 gage) with leakage less than the estimated detection limit of 0.02 cubic inch per hour (0.30 cm^3/hr). Inspection of the sealing surfaces revealed several local wear areas on the copper nose-

TABLE III. - OPERATIONAL PARAMETERS AND LEAKAGE RATES OF SEAL SEAT AND NOSEPIECE COMBINATIONS (SOFT ON HARD)

WITH ONE SURFACE HAVING A WEAR-IN OR CONFORMABILITY PROPERTY

[Condition of sealing surfaces unsatisfactory after each run.]

Run	Seal nosepiece	Seal seat	Sodium temperature		Sealed pressure		Sliding velocity		Operating time, hr	Leakage rate				Oxygen content, ppm
										$in.^3/hr$		cm^3/hr		
			^oF	^oC	psig	N/cm^2 gage	ft/sec	m/sec		Start	Stop	Start	Stop	
1	Titanium carbide - columbium carbide - tantalum carbide with 20 percent cobalt binder	Calcium fluoride - barium fluoride film on nickel-base alloy	1000	538	20.5	14.1	79	24	3.7	0.3	11	5.5	180	--
2	Tungsten carbide with 9-percent cobalt binder	Calcium fluoride - barium fluoride film on nickel-base alloy			7.0	4.8			.7	----	4	-----	60	85
3		Molybdenum			65.0	45.0			2.2	4.0	34	60	560	--
4		40-Volume-percent foam nickel with calcium fluoride - barium fluoride impregnate			9.5	6.6			.6	7.3	55	120	900	--
5		40-Volume-percent foam nickel with calcium fluoride - barium fluoride impregnate	950	510	15.4	10.6	39	12	1.5	16.0	57	270	930	--
6		50-Volume-percent foam nickel-base alloy with calcium fluoride - barium fluoride impregnate	900	482	19.7	13.6			1.7	27.0	26	450	430	--
7		40-Volume-percent foam nickel with calcium fluoride - barium fluoride impregnate	755	402	15.9	11.0			1.5	4.7	10	78	170	--
8			600	316	18.8	13.0			1.3	3.2	29	53	470	--
9	Aluminum oxide (Al_2O_3)		600	316	12.5	8.6			1.6	6.7	12	110	190	--
10	Copper	Molybdenum	Immediate failure											71
11	Copper	Tungsten carbide - 10 percent tantalum carbide	600	316	10.5	7.2	39	12	4.0	1.3	2.6	22	43	--

TABLE IV. - OPERATIONAL PARAMETERS AND LEAKAGE RATES FOR SPIRAL-GROOVE SEAL

Run	Nosepiece material	Seat seat material	Location of spiral groove	Sodium temperature		Sealed pressure		Sliding velocity		Leakage rate				Operating time, hr	Condition of seal surfaces after run
										$in.^3/hr$		cm^3/hr			
				°F	°C	psig	N/cm^2 gage	ft/sec	m/sec	Start	End	Start	End		
1	Copper	Titanium carbide	Nosepiece	375	190	20	14	30	9.1	(a)	(a)	(a)	(a)	4.0	Good
2	Copper	Molybdenum	Seal seat	425	218	20	14	48	15	(a)	(a)	(a)	(a)	7.0	Excellent
				500	260	20	14	64	20	0.02	0.02	0.3	0.3	2.0	
3	Copper	Molybdenum	Seal seat	500	260	20	14	64	20	(b)	(b)	(b)	(b)	4.0	Excellent

[a]Not detectable (limit of detection, ≈ 0.30 cm^3/hr (0.02 $in.^3/hr$)).

[b]Visual observation revealed leakage in the form of minute drops but leakage was below limit of detection.

piece; the major portion of the surface showed no evidence of rubbing contact (fig. 20).

Another assembly evaluated consisted of a plain copper nosepiece and a molybdenum spiral-groove seal seat. This combination was operated for 9 hours at various speeds and at a sodium pressure of 20 pounds per square inch gage (14 N/cm^2 gage) with negligible leakage. Visual observation of the seal below 64 feet per second (20 m/sec) indicated leakage of intermittent minute drops of liquid sodium which oxidized into small pepper-size flakes. (Visual observation required the opening of the enclosure; thus some oxygen was present around the seal area during the inspection.) Above 64 feet per second (20 m/sec) these drops could not be observed. The sealing surfaces were in excellent condition after the 9 hours of operation (fig. 21) and showed that rubbing contact had occurred over most of the surface (probably at startup). As mentioned previously, the combination of copper and molybdenum operated only 3 minutes in the conventional face seal configuration and showed extreme surface distress even though the temperature, pressure, and speed were lower. It was concluded that the spiral-groove seal operated with interface separation. This conclusion is based on the excellent surface condition of the copper and molybdenum surfaces and on the fact that this poor wear combination (copper on molybdenum) was operated successfully at a relatively high temperature of 500° F (260° C) and a speed of 64 feet per second (20 m/sec) for 9 hours in a poor boundary lubricant, sodium. Before startup, the seal showed no leakage; this indicated good contact and flatness at the sealing surfaces. At shutdown, the seal showed slight leakage at zero rotation which indicated that some change in surface flatness had occurred. It should be pointed out that leakage at zero rotation is a function of pressure and flatness of the sealing surfaces. Spiral grooves were also incorporated into carbide seal seats and were mated to carbide nosepieces (in four tests). Leakage results were similar to those in table IV, and sliding surfaces were in excellent condition after several hours of operation to 500° F (260° C) in liquid sodium.

Spiral seal arrangements. - Several spiral seal arrangements are possible as indicated in figures 22 and 23. On startup the pumping action of the spiral grooves displaces

the sodium inward (fig. 21) from the seal dam; thus the seal tends to become pressure loaded (fig. 7(a)). This pressure load must be offset by hydrodynamic forces to prevent excessive rubbing contact. It is postulated that hydrodynamic forces arise from a slider bearing effect of the spiral-groove land area and from the pressure patterns developed by the spiral grooves. (Reference 9 includes a discussion of viscoseal pressure patterns.) The two arrangements evaluated in this study concerned pressurized liquid at the inside diameter of the seal interface; one arrangement had spiral grooves on the nonrotating nosepiece, and the other had spiral grooves on the rotating seal seat. Arrangements which were not evaluated involved pressurized liquid at the outside diameter of the seal interface (fig. 23). In this latter case, centrifugal force works to prevent leakage, and low-leakage rates should be more readily attainable than in the arrangement with pressurized liquid at the inside diameter.

Comparison of spiral-groove face seal and helical viscoseal. - The spiral-groove face seal operates with the same sealing principle as the helical viscoseal (fig. 24). However, it is inherently more compact and in addition provides positive sealing at zero rotation. The helical viscoseal requires an additional positive contact seal to prevent leakage at startup, shutdown, or in a static condition. The pressure generating capacity of the helical viscoseal or spiral seal is given by reference 20 as

$$\frac{\Delta P}{L} = \frac{6U\mu(\lambda G)}{c^2} \tag{3}$$

where ΔP is the pressure differential across the seal, L the wetted seal length, U the peripheral speed, μ the absolute viscosity, λ the sealing coefficient, G the geometry factor, and c the clearance. It is pointed out that the pressure gradient is a function of c^2. In a spiral-groove face seal, a much smaller clearance c is more readily attained than with the cylindrical viscoseal. For example, a 0.005-inch (0.013-cm) radial clearance is required in some viscoseal designs because of shaft runout and vibration. But a spiral face seal probably operates with less than 0.0005-inch (0.0013-cm) clearance. Hence, the spiral-groove face seal is inherently smaller for the same application.

SUMMARY OF RESULTS

Conventional face contact seals and face contact seals incorporating the spiral-groove geometry were evaluated for leakage and wear when sealing liquid sodium. The following were the significant results:

1. In comparison with conventional face contact seals, the spiral groove seals

showed negligible leakage and wear. Hydrodynamic separation of the sealing surfaces is postulated.

2. Static leakage of the spiral-groove face seal was similar to that of a face contact seal.

3. As compared to the helical-groove seal, the spiral-groove face seal has the following advantages:

(a) It is more compact in size because of higher pressure capacity produced by the inherently smaller seal gap.

(b) It functions as a face contact seal at startup and for shutdown.

4. Successful low-leakage operation was not achieved with conventional face contact seals (no spiral grooves) having carbide seal rings (hard on hard combination). Thermal distortions coupled with the lack of conformability (high hardness and modulus) and the poor lubricating ability of the sodium caused wear and scoring of the sealing surfaces.

5. Successful low-leakage operation was not achieved with conventional face contact seals (no spiral grooves) having soft on hard material combinations which were used in an attempt to obtain some conformability to offset thermal distortions. Generally, the sealing dam surfaces showed better contact and less scoring than did the hard on hard combinations, but leakage was not lower.

Lewis Research Center,
National Aeronautics and Space Administration,
Cleveland, Ohio, January 3, 1967,
120-27-04-03-22.

REFERENCES

1. King, Alan E.: Screw Type Shaft Seals for Potassium Lubricated Generators. IEEE Trans. on Aerospace, vol. AS-3, June 1965, supplement, pp. 471-479.

2. Bisson, Edmond E.; and Anderson, William J.: Advanced Bearing Technology. NASA SP-38, 1964.

3. Granan, J. R.; and Kumpitsch, R. C.: Pumps for Liquid-Metal Flight Controls. Paper No. 66-FE-20, ASME, Apr. 1966.

4. Fournet, Gérard; and Bonnefille, Robert: New Electrical Machines. Int. Sci. Tech., no. 51, Mar. 1966, pp. 38-47.

5. Kelly, Robert W.; Wood, Glenn M.; and Manfredi, Daniel V.: Cermet Face Seals for Inert Gas Environments. Preprint No. 65 AM 4C4, ASLE, May 1965.

6. Hamilton, D. B.; Walowit, J. A.; and Allen, C. M.: A Theory of Lubrication by Microirregularities. J. Basic Eng., vol. 88, no. 1, Mar. 1966, pp. 177-185.

7. Nau, B. S.: Hydrodynamics of Face Seal Films. Proceedings of the Second International Conference on Fluid Sealing, Cranfield, England, April 6-8, 1964. B. S. Nau, H. S. Stephens, and D. E. Turnbull, eds., British Hydromechanics Research Association, 1964, pp. F5-61 to F5-80.

8. Pinkus, Oscar; and Sternlicht, Beno: Theory of Hydrodynamic Lubrication. McGraw-Hill Book Co., Inc., 1961.

9. Zuk, John; Ludwig, Lawrence P.; and Johnson, Robert L.: Flow and Pressure Field Analysis of Parallel Groove Geometry For an Incompressible Fluid With Convective Inertia Effects. NASA TN D-3635, 1966.

10. Jackson, Carey B., ed.: Liquid Metals Handbook. Sodium - NaK Supplement. Rep. No. TID-5277, AEC and Bureau of Ships, July 1, 1955.

11. Kuivinen, David E.: Determination of Oxygen in Liquid Alkali Metals by the Mercury Amalgamation Method. Paper presented at the Nineteenth Meeting, Chemical Rocket Propulsion Group, (St. Paul, Minn.), July-Aug. 1963.

12. Elliott, D. F.; Holland, E.; and Tomblin, K. A.: Some Preliminary Tests on Bearing Materials to Operate Under Liquid Sodium. Rep. No. AERE-R/R-1891, Research Establishment, Harwell, Berks., England, Apr. 23, 1956.

13. Jerman, R. B.; Williams, R. C.; and Leeser, D. O.: Evaluation of Material Wear and Self-Welding in Sodium-Cooled Reactor Systems. J. Basic Eng., vol. 81, no. 2, June 1959, pp. 213-225.

14. Lyman, Taylor, ed.: Properties and Selection of Metals. Vol. 1 of Metals Handbook. 8th ed., American Society for Metals, 1961.

15. Coffin, L. F., Jr.: Boundary Lubrication, Wear-In and Hydrodynamic Behavior of Bearings for Liquid Metals and Other Fluids. ASLE Trans., vol. 1, no. 1, Apr. 1958, pp. 139-150.

16. Kissel, J. W.; Glaeser, W. A.; and Allen, C. M.: Sliding Contact Frictional Behavior in Sodium Environments. ASLE Trans., vol. 5, no. 1, Apr. 1962, pp. 39-44.

17. Balchin, N. C.: The Friction of Clean Metals Immersed in Liquid Sodium. Brit. J. Appl. Phys., vol. 13, Nov. 1962, pp. 564-569.

18. Sliney, Harold E.; Strom, Thomas N.; and Allen, Gordon P.: Fused Fluoride Coatings as Solid Lubricants in Liquid Sodium, Hydrogen, Vacuum, and Air. NASA TN D-2348, 1964.

19. Timoshenko, S.: Strength of Materials. Part II. 3rd ed., D. Van Nostrand Co., Inc., 1956.

20. Ludwig, Lawrence P.; Strom, Thomas N.; and Allen, Gordon P.: Gas Ingestion and Sealing Capacity of Helical Groove Fluid Film Seal (Viscoseal) Using Sodium and Water as Sealed Fluids. NASA TN D-3348, 1966.

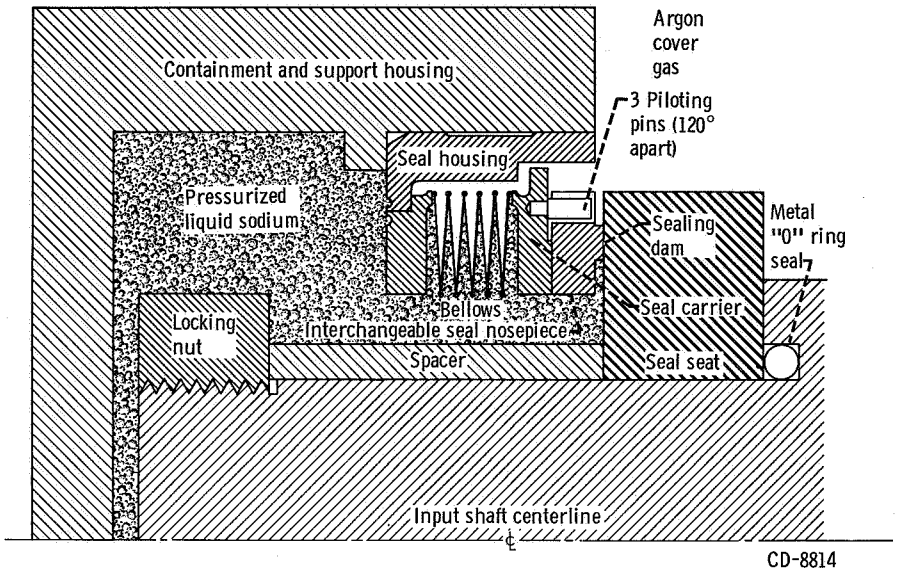

Figure 1. - Schematic diagram of face contact seal assembly and experimental apparatus.

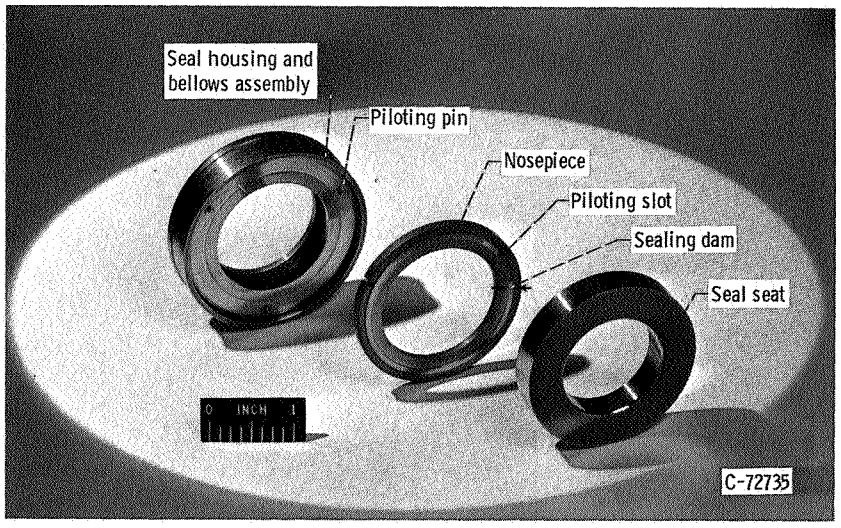

Figure 2. - Face contact seal.

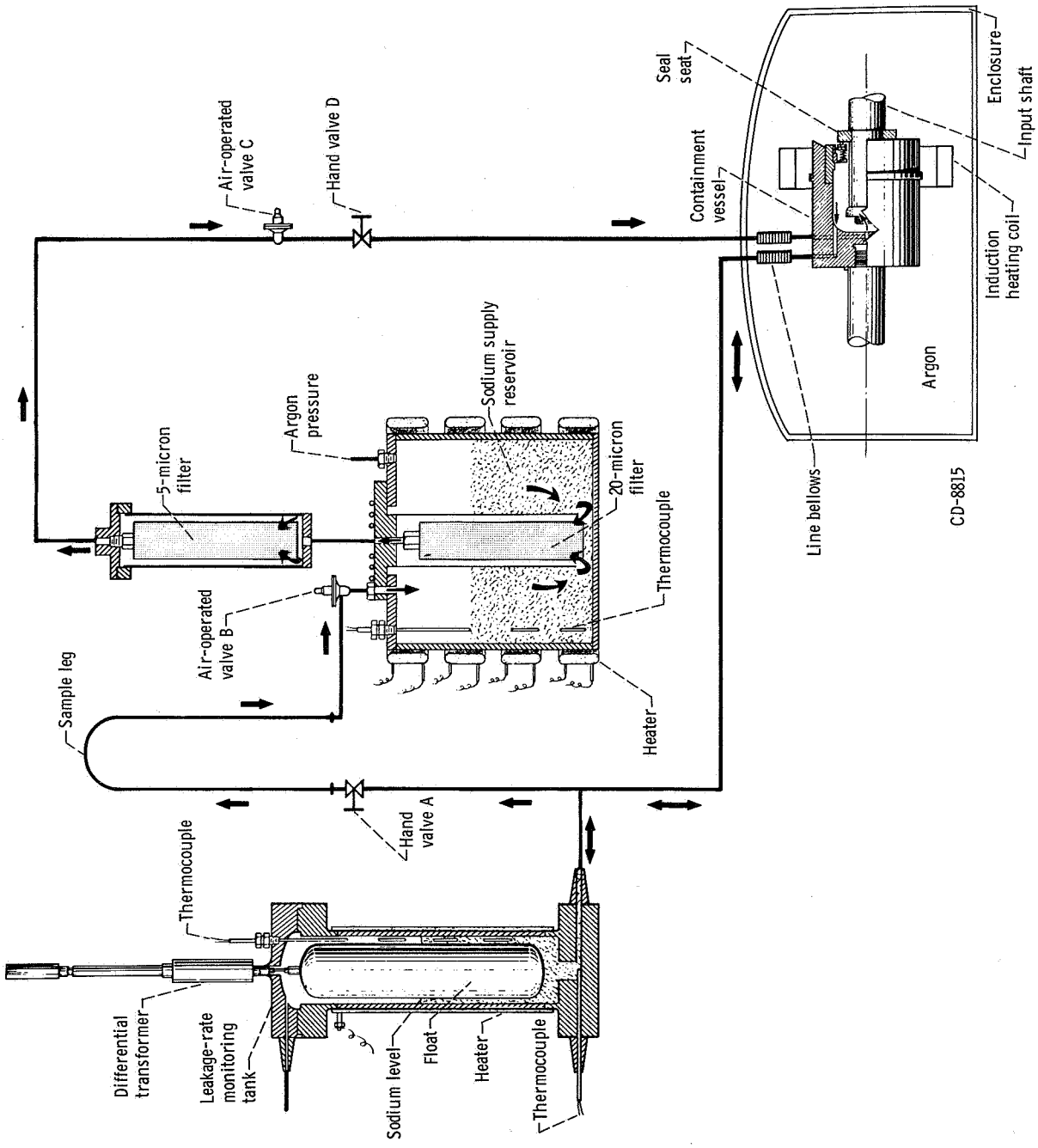

Figure 3. - Sodium supply system.

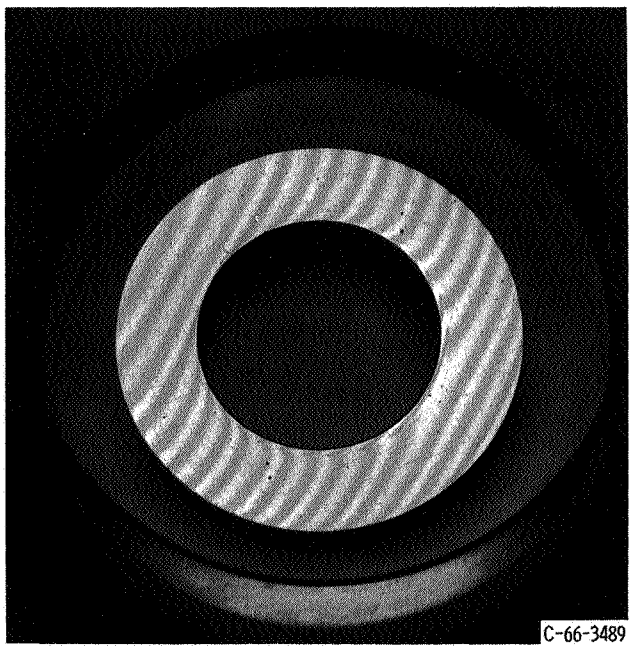

Figure 4. - Light interference patterns showing surface flatness typical of carbide seal seats.

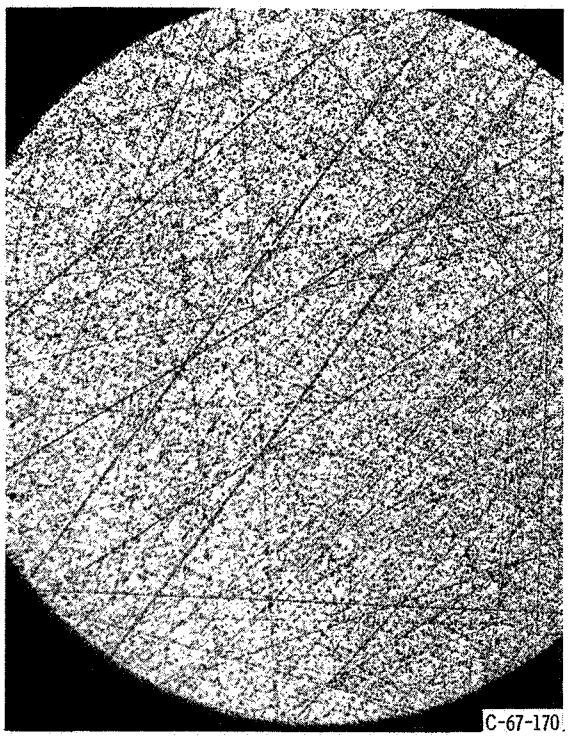

(a) Photomicrograph of surface. X100.

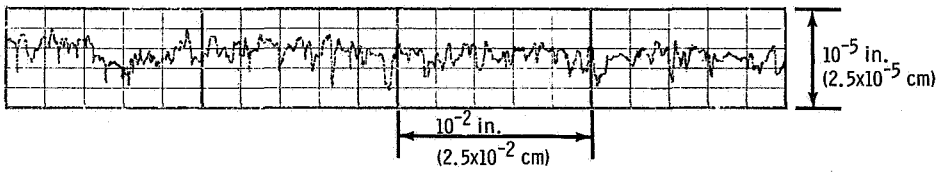

(b) Surface profile.

Figure 5. - Typical surface condition of tungsten carbide seal seat before operation in sodium.

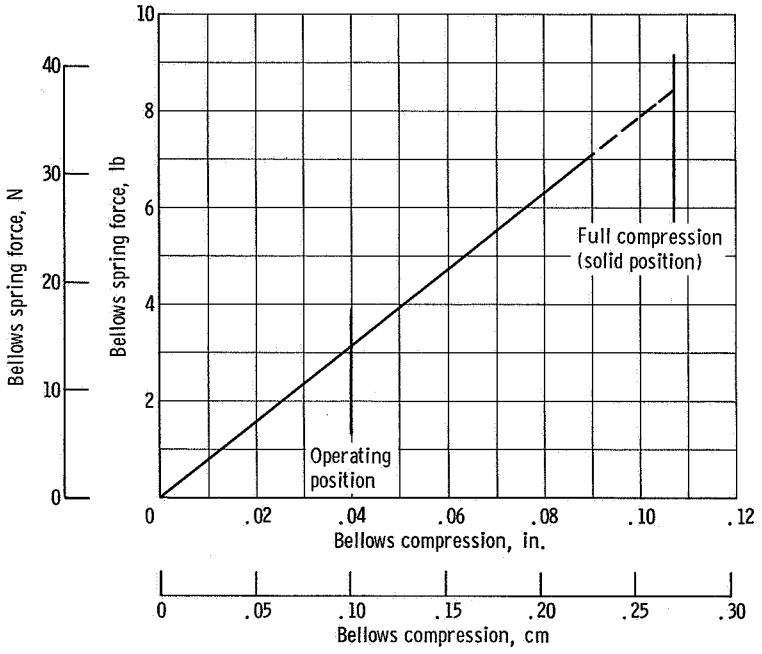

Figure 6. - Calibration of bellows spring force with bellows compression.

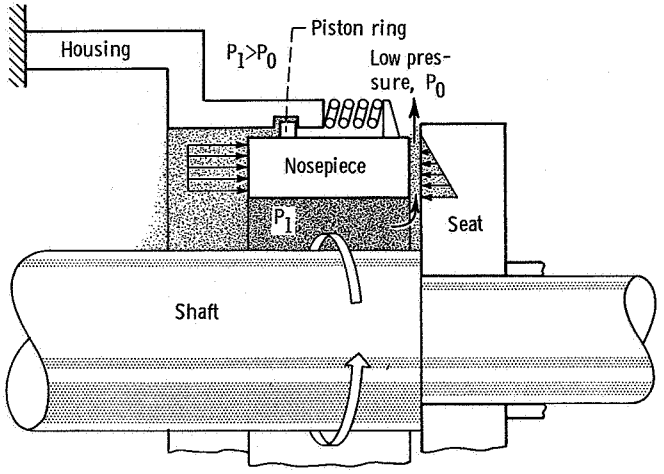

(a) Pressure loaded.

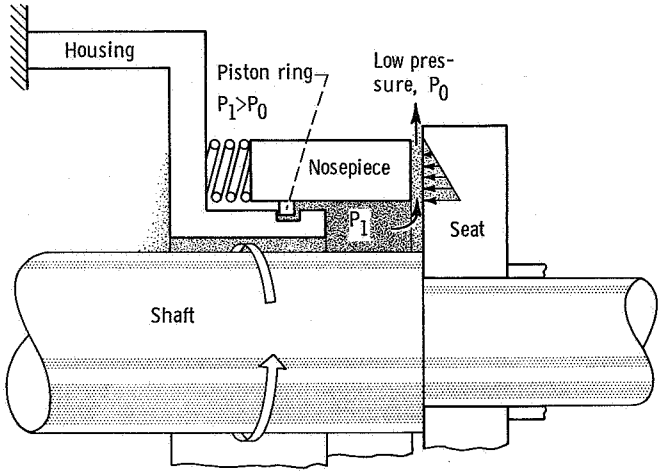

(b) Pressure unloaded.

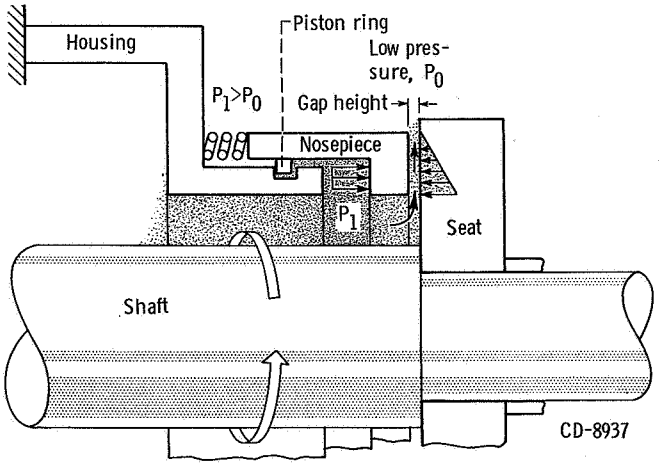

(c) Pressure balanced.

Figure 7. - Face contact seal pressure balance.

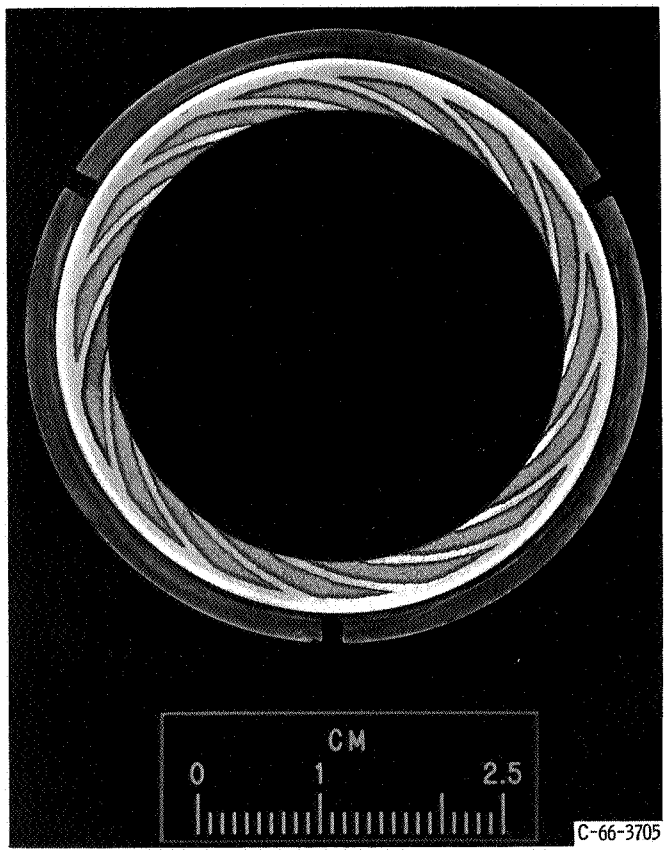

Figure 8. - Spiral-groove geometry chemically etched into copper nosepiece.

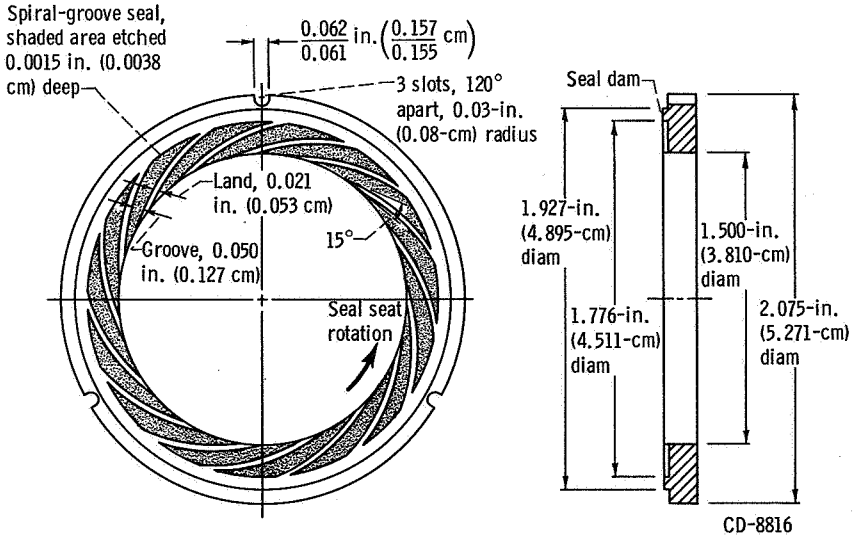

Figure 9. - Spiral-groove and nosepiece geometry.

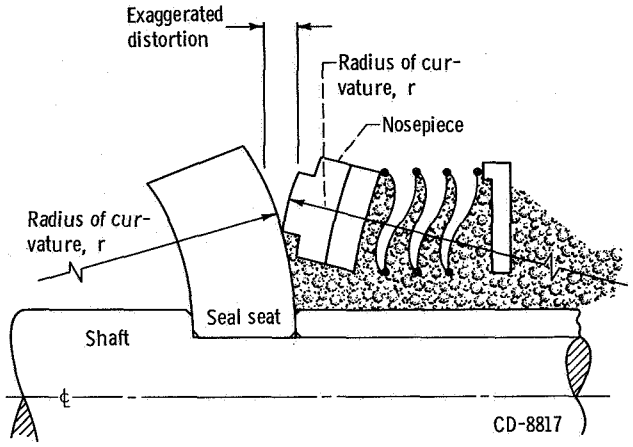

Figure 10. - Schematic diagram showing edge contact caused by axial thermal gradients.

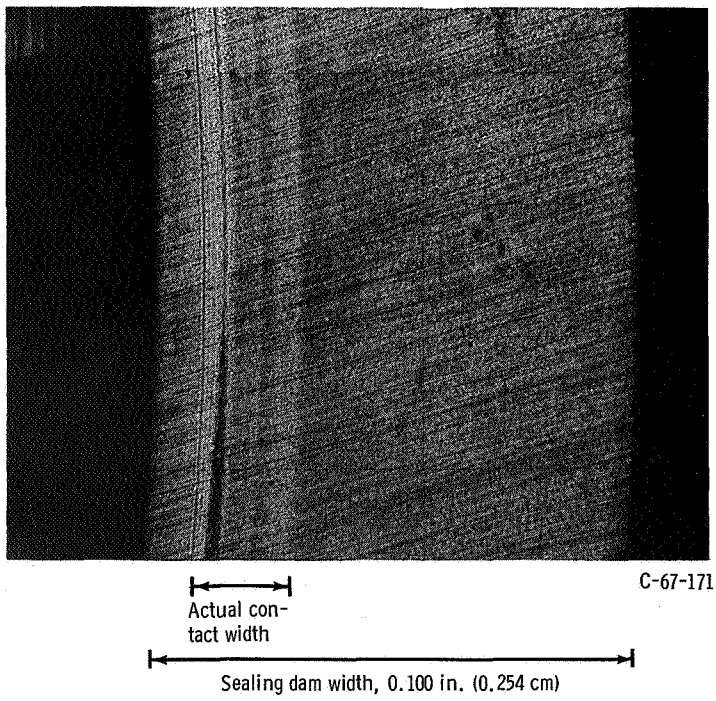

(a) Photomicrograph of surface.

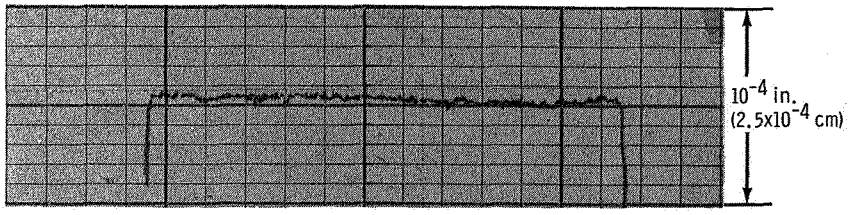

(b) Surface profile.

Figure 11. - Photomicrograph and surface profile of titanium carbide nosepiece after operation against tungsten carbide seal seat showing limited contact width. Sodium temperature, 740° F (393° C); operating time, 40 minutes; sliding velocity, 79 feet per second (24 m/sec); pressure, 30 pounds per square inch gage (20.6 N/cm^2 gage).

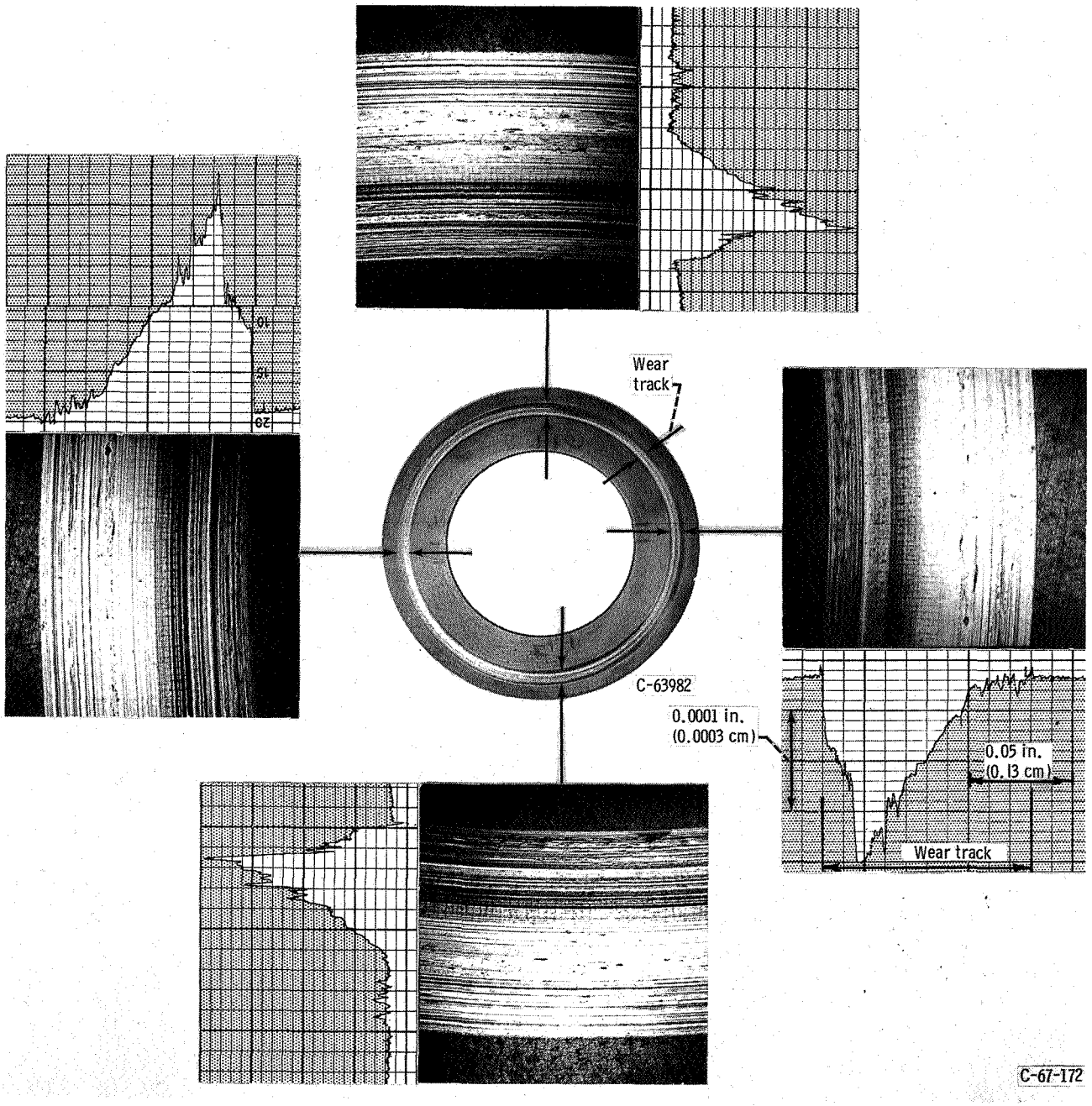

Figure 12. - Overall wear pattern, surface profile traces, and photomicrographs of tungsten carbide seal seat. Sodium temperature, 1000° F (538° C); operating time, 4 hours; sliding velocity, 79 feet per second (24 m/sec); pressure, 50 pounds per square inch gage (34 N/cm^2 gage).

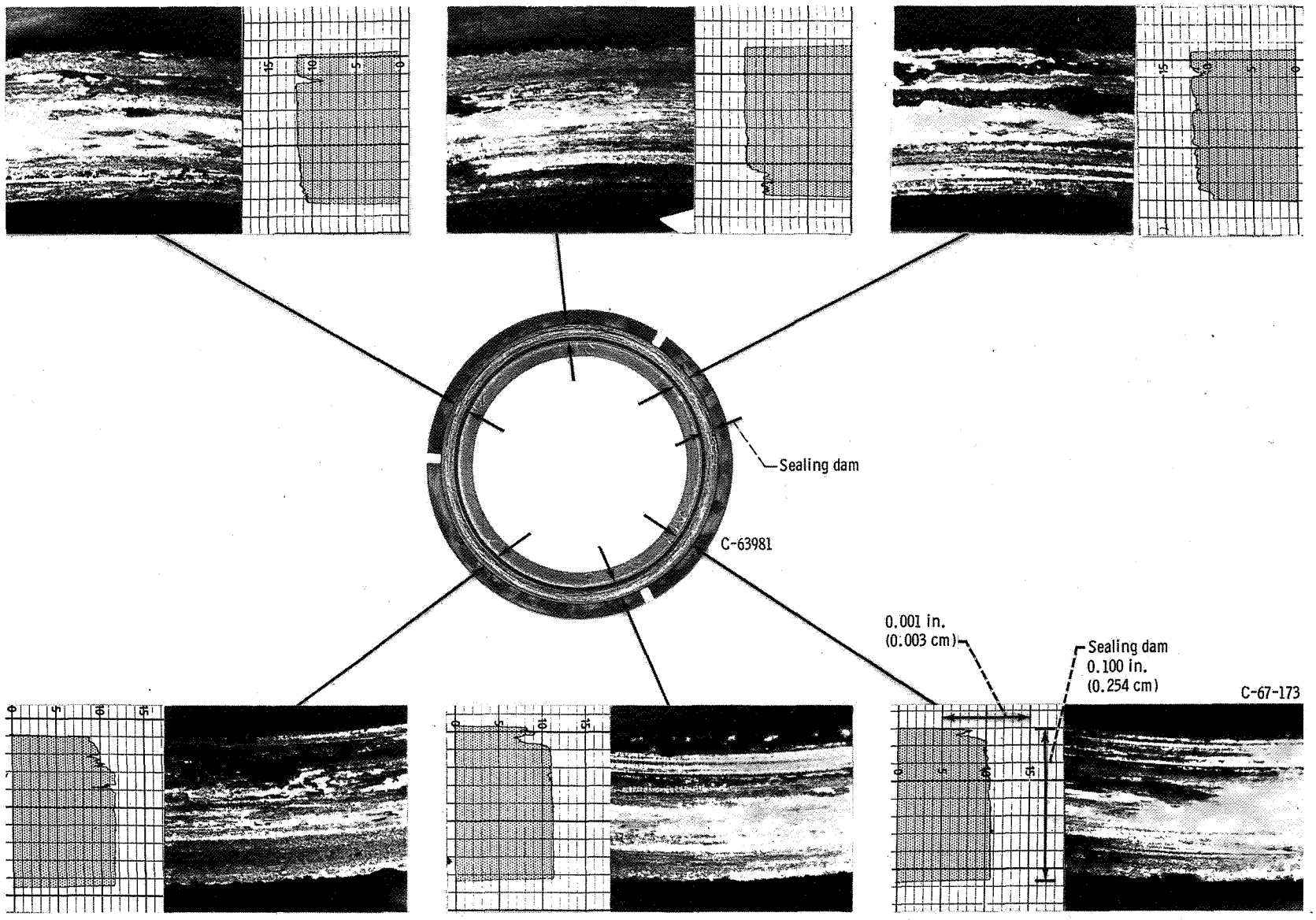

Figure 13. - Overall wear pattern, surface profile traces, and photomicrographs of titanium carbide seal seat. Sodium temperature, 1000° F (538° C); operating time, 4 hours; sliding velocity, 79 feet per second (24 m/sec); pressure, 50 pounds per square inch gage (34 N/cm^2 gage).

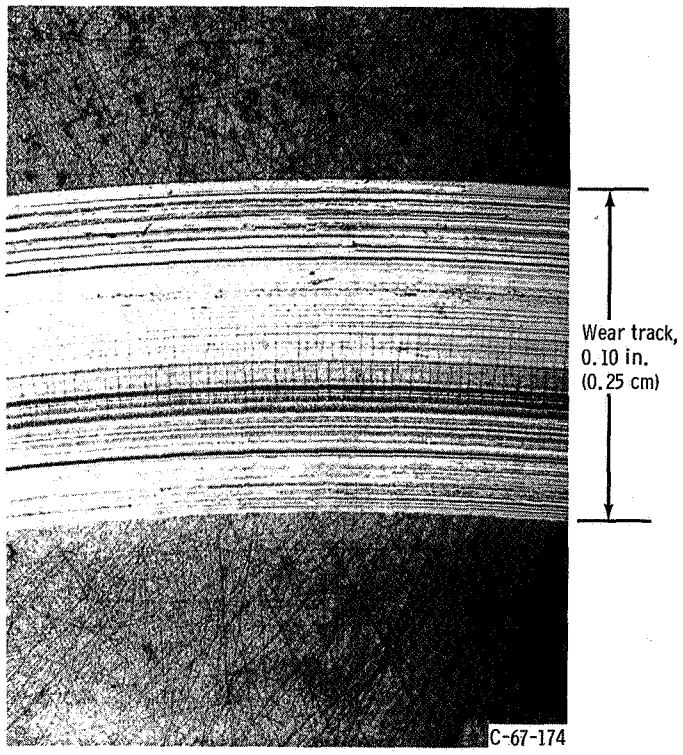

Figure 14. - Photomicrograph of tungsten carbide seal seat showing heavy scoring and heat checking. Sealed fluid, sodium; sodium temperature, 1000° F (538° C); sliding velocity, 79 feet per second (24 m/sec); sealed pressure, 50 pounds per square inch gage (34 N/cm^2 gage); mating material, titanium carbide - niobium carbide - tantalum carbide composite.

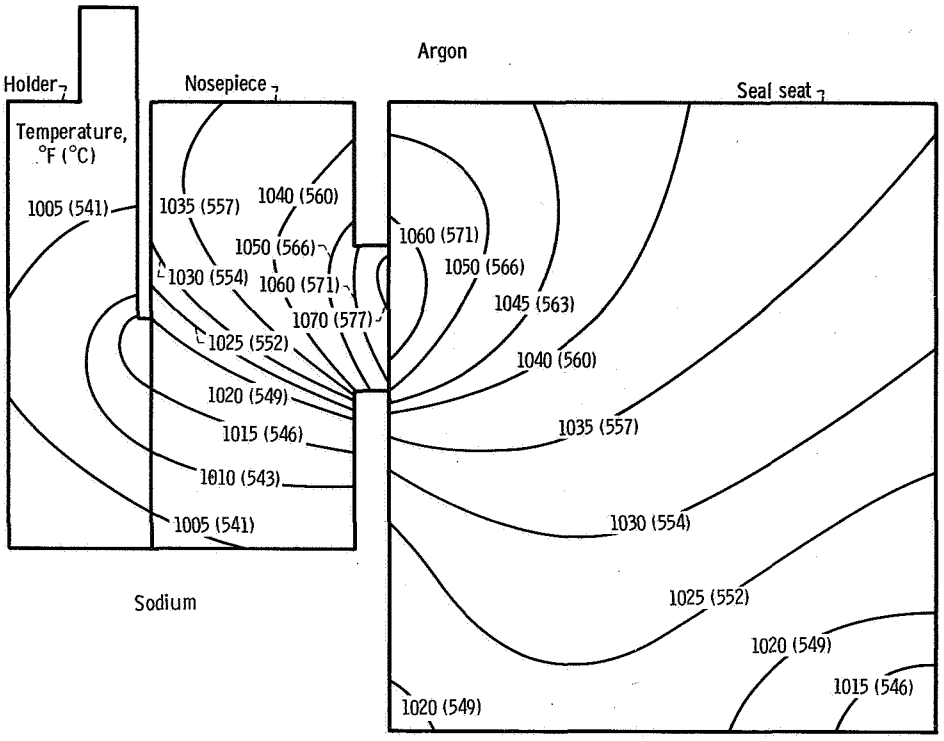

(a) Nonbeveled design.

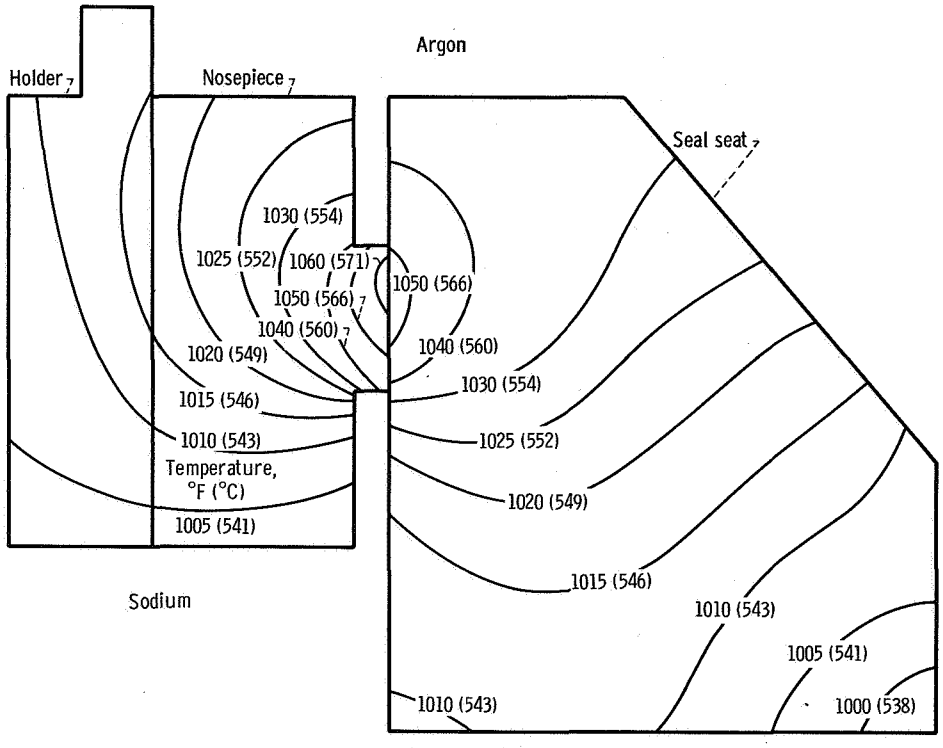

(b) Beveled design.

Figure 15. - Calculated thermal gradients in seal seat and nosepiece. Tungsten carbide seal seat; titanium carbide nosepiece; sodium temperature, 1000° F (538° C); argon temperature, 360° F (182° C); sliding velocity, 79 feet per second (24 m/sec).

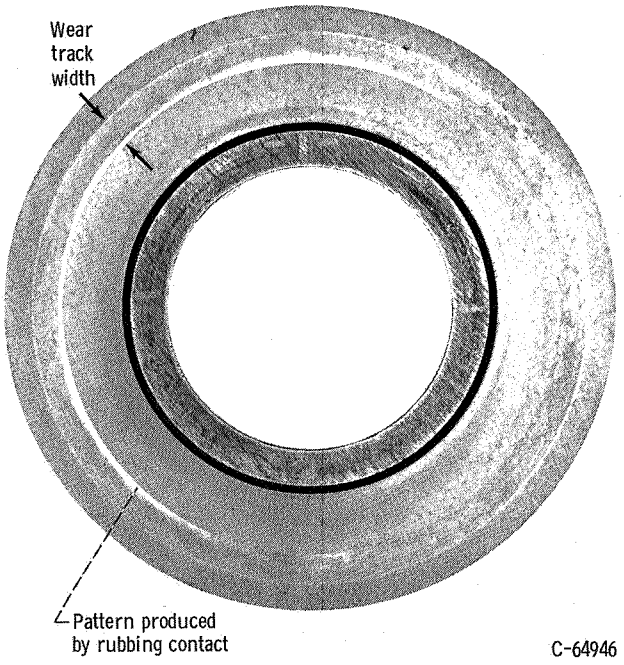

Figure 16. - Tungsten carbide seal seat showing wear pattern resulting from surface waviness. Sodium temperature, 1000° F (538° C); sliding velocity, 79 feet per second (24 m/sec); pressure, 50 pounds per square inch gage (34 N/cm^2 gage).

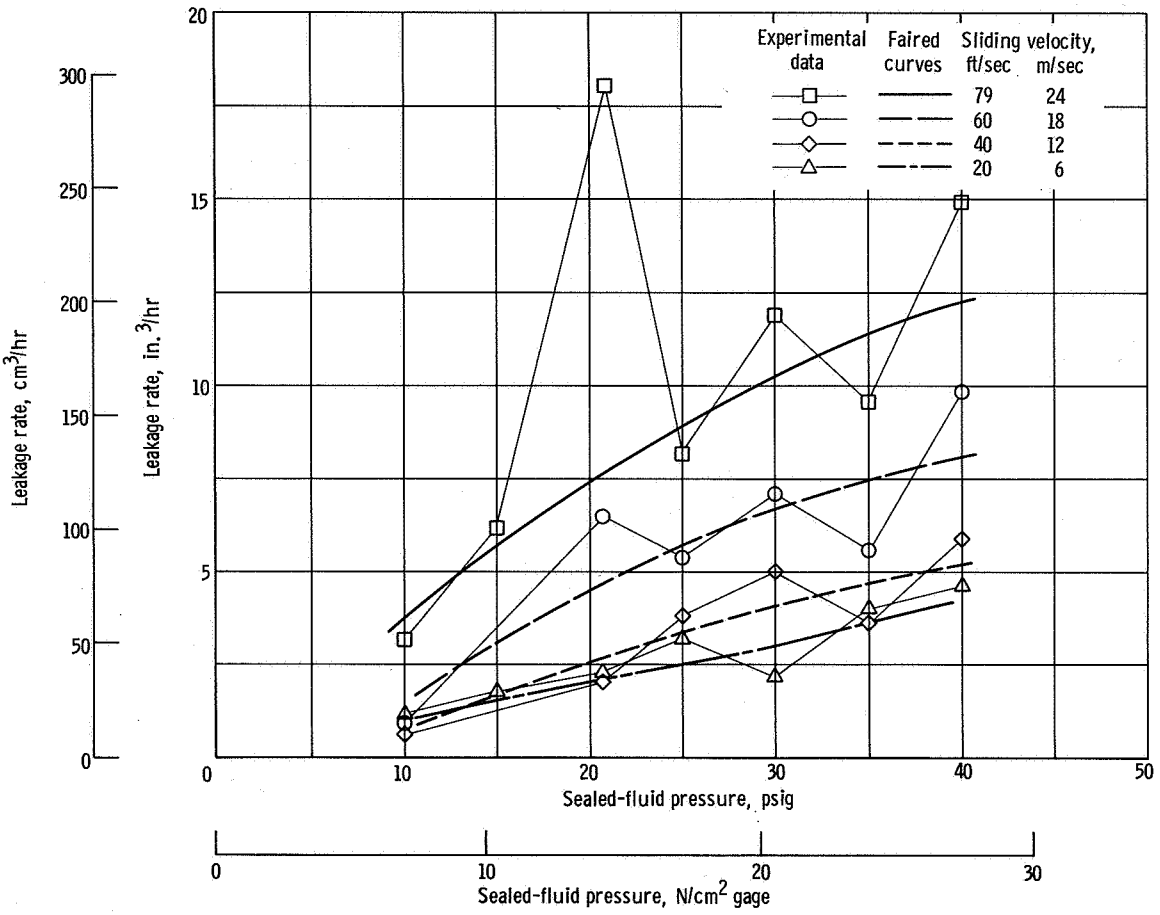

Figure 17. - Effect of speed and pressure on face-contact-seal leakage trends. Temperature, 600° F (316° C); tungsten-carbide seal seats and nosepieces; sealed fluid, sodium.

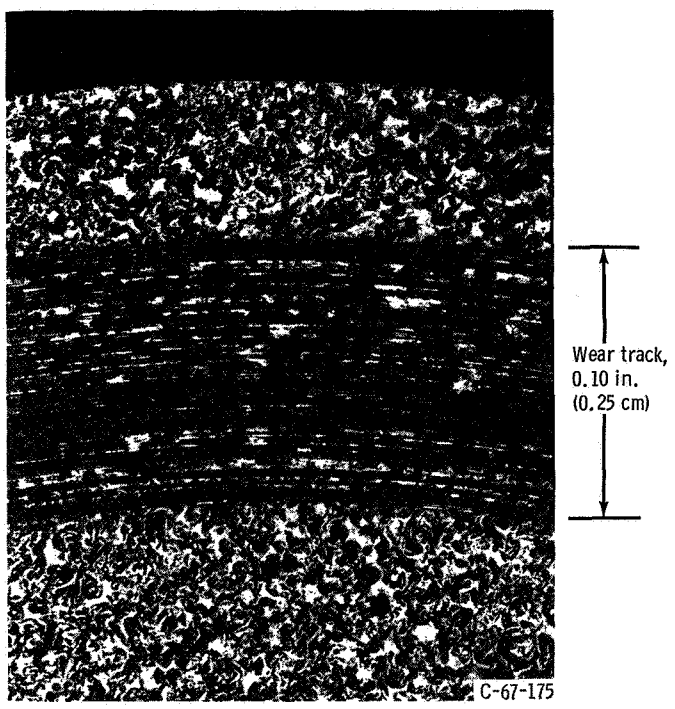

Figure 18. - Wear track on seal seat of 40-weight-percent foam nickel impregnated with calcium fluoride - barium fluoride. Sealed fluid, sodium; sodium temperature, 1000° F (538° C); sliding velocity, 79 feet per second (24 m/sec); sealed pressure, 9.5 pounds per square inch gage (6.6 N/cm^2 gage).

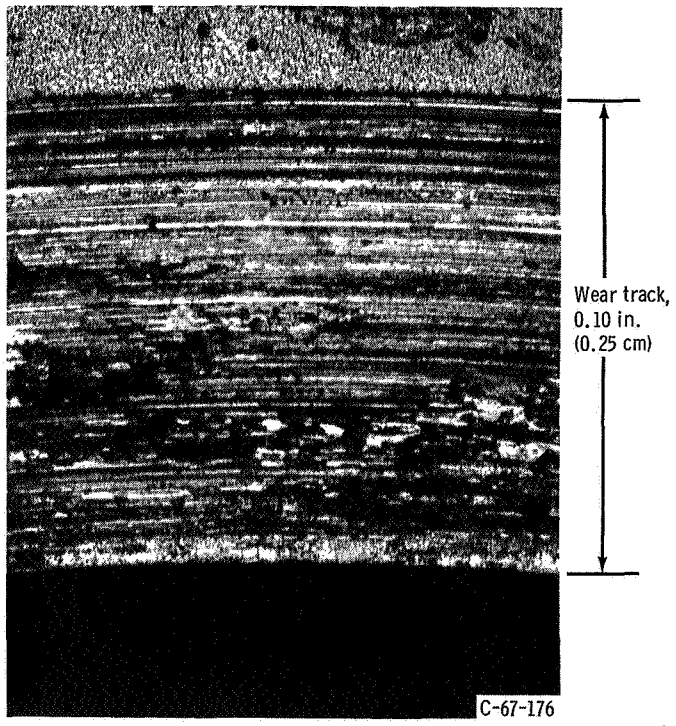

Figure 19. - Wear track on molybdenum seal seat. Sealed fluid, sodium; sodium temperature, 1000° F (538° C); sliding velocity, 79 feet per second (24 m/sec); sealed pressure, 65 pounds per square inch gage (45 N/cm^2 gage).

(a) Local wear area.

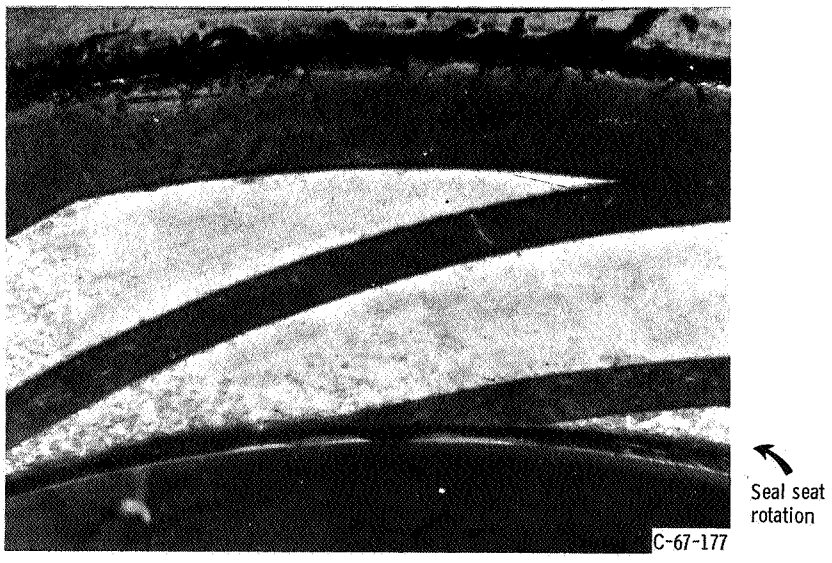

(b) Area showing no evidence of wear. (Typical of most of the sliding interface.)

Figure 20. - Seal nosepiece with inward-pumping spiral-groove design. Material, copper; sealed fluid, sodium; sodium temperature, 400° F (204° C); operating time, 4 hours; sliding velocity, 35 feet per second (11 m/sec); sealed pressure, 20 pounds per square inch gage (14 N/cm^2 gage).

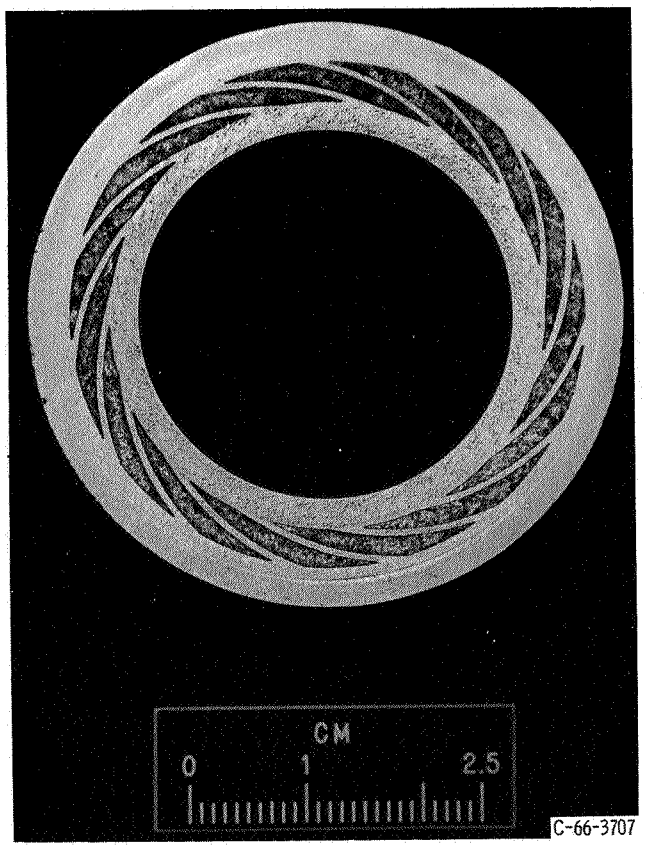

Figure 21. - Spiral-groove geometry chemically etched into molybdenum seal seat.

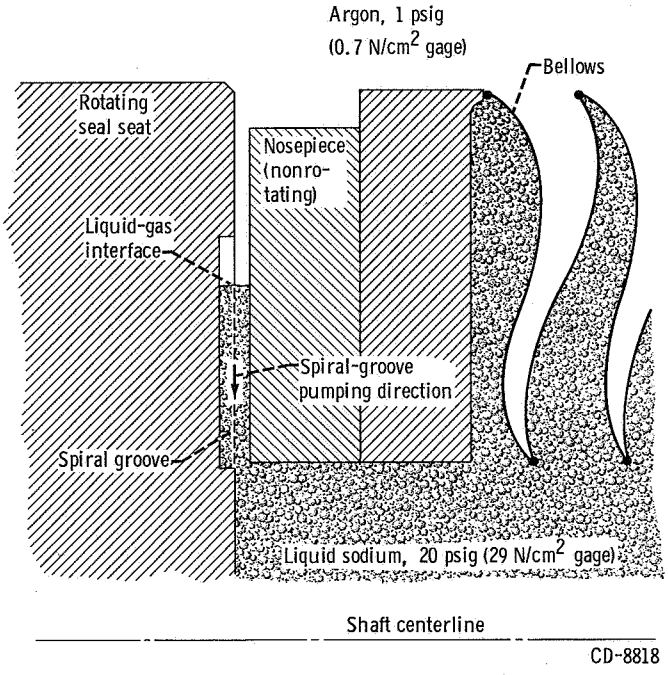

Figure 22. - Spiral-groove seal seat in operating mode.

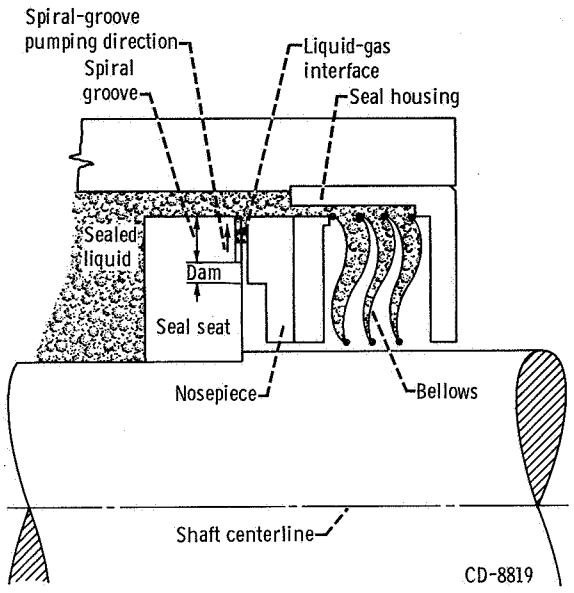

Figure 23. - Spiral-groove placement in seal seat for sealing liquid at outside diameter of seal dam.

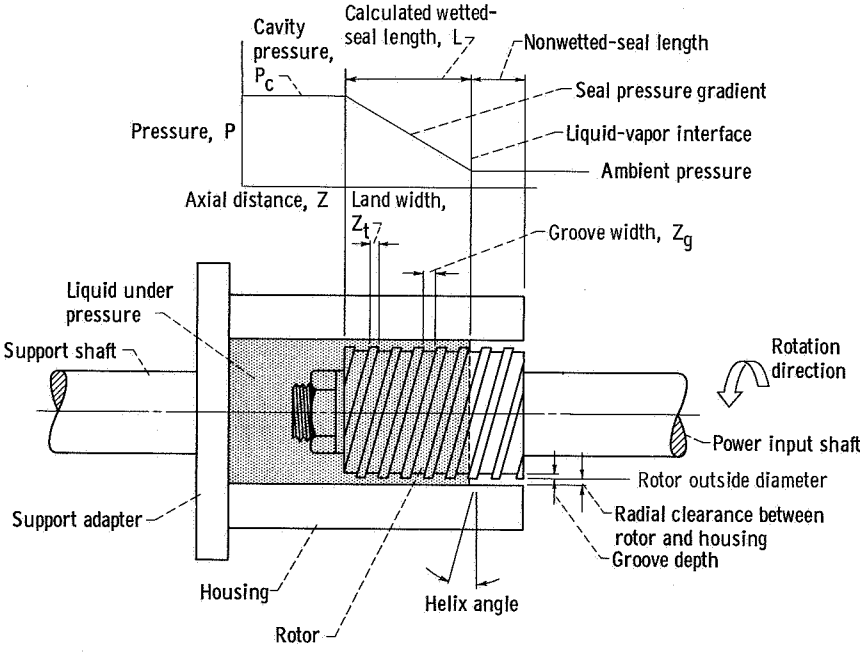

Figure 24. - Helical-groove rotor viscoseal.

19/5/67

"The aeronautical and space activities of the United States shall be conducted so as to contribute . . . to the expansion of human knowledge of phenomena in the atmosphere and space. The Administration shall provide for the widest practicable and appropriate dissemination of information concerning its activities and the results thereof."

—NATIONAL AERONAUTICS AND SPACE ACT OF 1958

NASA SCIENTIFIC AND TECHNICAL PUBLICATIONS

TECHNICAL REPORTS: Scientific and technical information considered important, complete, and a lasting contribution to existing knowledge.

TECHNICAL NOTES: Information less broad in scope but nevertheless of importance as a contribution to existing knowledge.

TECHNICAL MEMORANDUMS: Information receiving limited distribution because of preliminary data, security classification, or other reasons.

CONTRACTOR REPORTS: Scientific and technical information generated under a NASA contract or grant and considered an important contribution to existing knowledge.

TECHNICAL TRANSLATIONS: Information published in a foreign language considered to merit NASA distribution in English.

SPECIAL PUBLICATIONS: Information derived from or of value to NASA activities. Publications include conference proceedings, monographs, data compilations, handbooks, sourcebooks, and special bibliographies.

TECHNOLOGY UTILIZATION PUBLICATIONS: Information on technology used by NASA that may be of particular interest in commercial and other non-aerospace applications. Publications include Tech Briefs, Technology Utilization Reports and Notes, and Technology Surveys.

Details on the availability of these publications may be obtained from:

SCIENTIFIC AND TECHNICAL INFORMATION DIVISION

NATIONAL AERONAUTICS AND SPACE ADMINISTRATION

Washington, D.C. 20546